# Communication between $Co_2(CO)_4$dppm Units via Polyferrocenylalkyne Linkages

Leigh-Anne Hore, C. John McAdam, Joy L. Kerr, Noel W. Duffy, Brian H. Robinson,* and Jim Simpson

*Department of Chemistry, University of Otago, P.O. Box 56, Dunedin, New Zealand*

*Received June 13, 2000*

The synthesis and characterization of a family of ethynylbi- and ethynylterferrocenyls, I−$Fc_2C{\equiv}CR$, $Fc_2C{\equiv}CR$, and $Fc_2(C{\equiv}CR)_2$ (R = Fc, $SiMe_3$), I−$Fc_3C{\equiv}CSiMe_3$, $Fc_3C{\equiv}CSiMe_3$, $Fc_3(C{\equiv}CSiMe_3)_2$, and their $Co_2(CO)_6$ and $Co_2(CO)_4$dppm complexes are described. The structure adopted by $Fc_2\{[Co_2(CO)_4\text{dppm } C_2SiMe_3]\}_2$ minimizes the steric interactions between the biferrocene and dppm moieties. Electrochemical studies show that identical redox centers—ferrocenyl termini, $Co_2(CO)_4$dppm units, or ferrocenyl groups in the core—communicate independently with each other.



## Introduction

Considerable attention has been given recently to molecules containing highly conjugated organometallic systems, especially those with multiple electroactive centers joined by a conjugated assembly. These compounds are of interest for their potential application in the construction of molecular scale electronic devices or the manifestation of advantageous bulk properties such as catalytic activity, large nonlinear optical responses, magnetism, and electron transfer.[1] Molecules that contain ligands with switchable redox behavior add another dimension. Our interest is the integration of switchable electrophores into arrays containing fluorescent centers. The link, which must be capable of transmitting the electronic effects while maintaining stereochemical control, is a crucial component of this module. In this paper we focus on possible links which can also function as electrophores: polyferrocenyl−C≡C− or polyferrocenyl−$C_2[Co_2(CO)_4$dppm].

Ferrocene, because of its simple redox behavior,[2] is a ubiquitous moiety wherever an electrophore is required, and it has played a major role in molecular sensors, electrochemical agents, liquid crystals, and nonlinear optical material development.[3] Biferrocene is another potential electrophore. Its redox chemistry, which displays two reversible one-electron couples, has attracted attention for many years, and electronic communication between the two $Fc^{+/0}$ couples is well established.[4] Electron transfer rates and charge delocalization of alkylated biferrocenium salts have been studied,[5a] and the crystal structure of a mixed valence salt revealed nonequivalence in the ferrocenyl moieties.[5b] Since both symmetrical and asymmetrical biferrocene derivatives are accessible, it has the added advantage of bringing to bear environmental factors to the magnitude of communication in the array. Thus biferrocene compounds can be utilized as both links and redox centers. Polyferrocenes are less well understood, the main reason being the difficulty in controlling syntheses of functionalized derivatives, although a series of alkylpolyferrocenes has been reported recently.[6] Our strategy was to start with a simple ferrocene compound and assemble the polyferrocene in a coherent synthetic sequence. A useful template is a ferrocenylalkynyl unit. First, the synthetic methodology for alkyne elaboration is well established. Second, unbranched ethynyl or polyalkynyl links appear from both experimental and theoretical work to be very efficient communicators; this connectivity is unaffected by the aromaticity of an interpolated group.[7] Third, the alkyne allows the addition of other electroactive centers. In particular, we have shown that coordination of a $Co_2(CO)_xL_y$ fragment across the −C≡C− bond provides a tunable redox center, as the electron density in the relevant redox orbitals can be varied by changing L.[8,9] The $Co_2(CO)_4$dppm fragment is especially important as, due to "clamping" of the Co−Co bond by the dppm, it is not affected by the fast ECE reactions

(1) (a) *Conjugated Polymer Materials: Opportunities in Electronic, Optoelectronic and Molecular Electronics*; Bredas, J. L., Chance, R. R, Eds.; NATO ASI Series, Vol. 182; Kluwer: Dordrecht, 1990. (b) Manners I. *R. Soc. Chem. Annu. Rep.−Inorg. Chem.* **1994**, *91*, 131.

(2) Zanello P. In *Ferrocenes*; Togni, A., Hayashi, T., Eds.; VCH: Weinheim, 1995; Chapter 7.

(3) (a) Togni, A. In *Ferrocenes*; VCH: Weinheim, 1995; Chapter 8. (b) Deschenaux, P.; Goodby, J. W. In *Ferrocenes*; VCH: Weinheim, 1995; Chapter 9.

(4) (a) Brown, G. M.; Meyer, T. J.; Cowan, D. O.; Le Vanda, C.; Kaufman, F. J.; Roling, P. V.; Rausch, M. D. *Inorg. Chem.* **1975**, *14*, 506. (b) Cowan, D. O.; Le Vanda, C.; Park, J.; Kaufman, F. J. *Acc. Chem. Res.* **1973**, *6*, 1. (c) Muller-Westerhoff, U. T. *Angew. Chem., Int. Ed. Engl.* **1986**, *25*, 702.

(5) (a) Hendrickson, D. N.; Oh, S. M.; Dong, T.-Y.; Kambara, T.; Cohn, M. J.; Moore, M. F. *Comments Inorg. Chem.* **1985**, *4*, 329. (b) Delville, M.-H.; Robert, F.; Gouzerh, P.; Linares, J.; Boukheddaden, K.; Varret, F.; Astruc, D. *J. Organomet. Chem.* **1993**, *451*, C10.

(6) (a) Dong, T.-Y.; Lee, W.-Y.; Su, P.-T.; Chang, L.-S.; Lin, K.-J. *Organometallics* **1998**, *17*, 3323. (b) Dong, T.-Y.; Ho, P.-H.; Lai, X.-Q.; Lin Z−W.; Lin, K.-J. *Organometallics* **2000**, *19*, 1096.

(7) Duffy, N. W.; McAdam, C. J.; Nervi, C.; Osella, D.; Ravera, M.; Robinson, B. H.; Simpson, J. *Inorg. Chim. Acta* **1996**, *247*, 99.

(8) Robinson, B. H.; Simpson, J. In *Paramagnetic Organometallic Species in Activation/Selectivity Catalysis*; Chanon, M. Ed.; Klymer: Durdrecht, 1989; p 357.

(9) McAdam, C. J.; Duffy, N. W.; Robinson, B. H.; Simpson, J. *Organometallics* **1996**, *16*, 3935. McAdam, C. J.; Duffy, N. W.; Robinson, B. H.; Simpson, J. *J. Organomet. Chem.* **1997**, *527*, 179. Duffy, N. W.; McAdam, C. J.; Robinson, B. H.; Simpson, J. *J. Organomet. Chem.* **1998**, *565*, 19. Duffy, N. W.; McAdam, C. J.; Robinson, B. H.; Simpson, J. *J. Organomet. Chem.* **1999**, *573*, 36.

(10) Arewgoda, M.; Rieger, P. H.; Robinson, B. H.; Simpson, J. *J. Am. Chem. Soc.* **1982**, *104*, 5633.

10.1021/om000493g CCC: $19.00 
Publication on Web 10/27/2000

**Scheme 1**

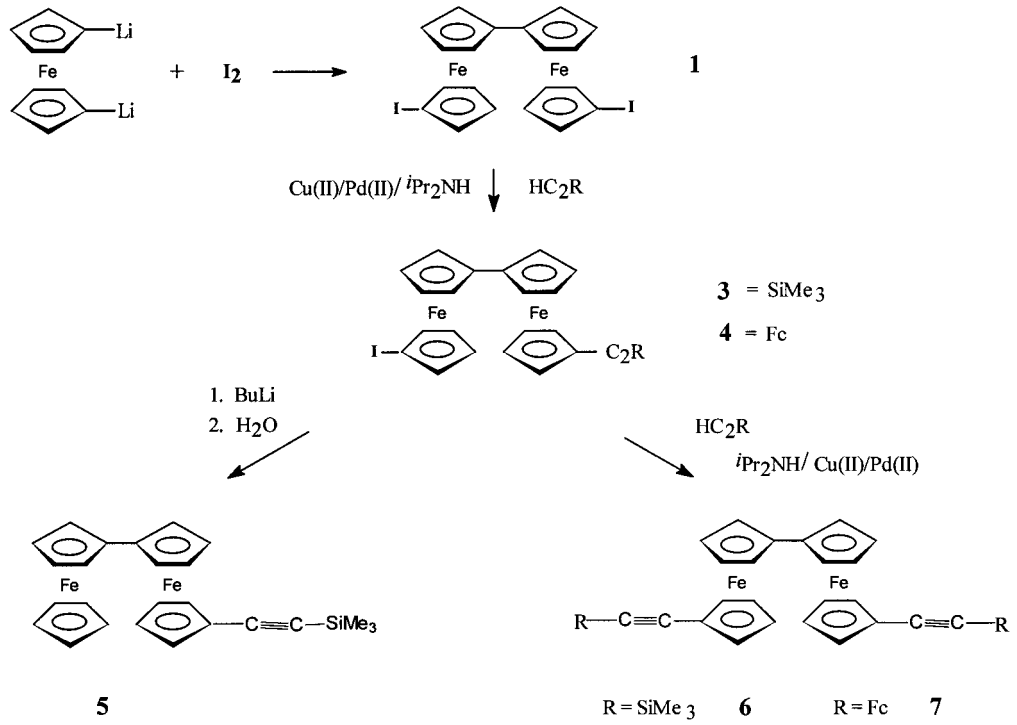


seen with many other alkynedicobalt carbonyl redox centers.[10] This clean oxidation response provides a probe for estimating the efficiency of communication along the array.

Long and co-workers have reported recently[11] both ethynyl and organometallic derivatives of biferrocene as precursors for materials having advantageous nonlinear optical behavior. 1′,6′-Bis(trimethylsilylethynyl)-biferrocene provided the route to the acetylides 1′,6′-bis{manganese(I)tricarbonyl[1,2-bis(diphenylphosphino)-methane}biferrocene and 1′,6′-bis{chlororutheniumbis-(diphenylphosphino)methane}biferrocene. Electrochemical data showed that the organometallic moiety donated electron density through the −C≡C− connection, which stabilized the Fe(II) center toward oxidation but decreased the relative stability of the Fe(II)Fe(III) mixed valence species.[11] A restriction on the versatility of their synthetic route is the low yield and unpredictable syntheses of $Fc_2I_2$.[12] Our intention was to adapt the iodination of ferrocene and lithioferrocene so that polyferrocene complexes with −C≡C− bonds could be prepared in quantities suitable for further incorporation into fluorescent arrays. This paper describes biferrocene and terferrocene linkages with or without cluster redox centers and with $Me_3Si$ or ferrocene end-groups.

## Results and Discussion

**Synthesis.** The two strategic reagents were diiodobiferrocene **1** and diiodoterferrocene **2**. Rausch,[12] Long,[11] and their co-workers have reported the preparation of **1** from FcLi. In our experience the yields were quite variable, and iodinated polyferrocenes were also produced in this reaction. We therefore investigated the effect of the relative mole ratio of iodine to lithiated ferrocene on the product composition. It was found that by varying the ratio of iodine to ferrocene it was possible to control whether $Fc_2I_2$ or terferrocenyliodides "$Fc_3I_x$" were the major products. Chromatographic separation of the iodinated $Fc_3$ compounds proved difficult with the added complication that they degrade on silica or alumina. The major $Fc_3$ component was **2**, which was the key reagent for further controlled elaboration of the polyferrocene backbone. In practice, it was convenient to utilize the crude "$Fc_3$" mixture in reactions with alkynes, as the products were much easier to separate.

Cu(I)/Pd(II)-catalyzed coupling of a terminal alkyne to **1** gave the desired ethynylbiferrocene (Scheme 1). An important step forward was the ability to control the coupling reaction with **1** and HC≡CR (R = $SiMe_3$, Fc), as this enabled the iodoethynylbiferrocenes **3** and **4** to be isolated in reasonable yield. Compound **3** is potentially a useful synthon for elaboration of the ferrocenyl framework. Thus, coupling of **3** with HC≡CR gave the target bisethynylferrocenes **6** (R = $SiMe_3$) and **7** (R = Fc) in good yields (Scheme 1). Long and co-workers[11] had previously prepared the bis-ethynyl complex **6** directly from **1**. Furthermore, the lithiation of **3** and quenching with water gave the mono-ethynyl derivative **5**.

The coupling reaction between **2** and trimethylsilylacetylene gave **8**, the terferrocene analogue of **3**, but it was moderately unstable and was only characterized spectroscopically. The mono-ethynyl **9** and bis-ethynyl **10** complexes were prepared from coupling reactions similar to those described above for the biferrocene derivatives (Scheme 2). Similar reactions with ethynylferrocene appeared to give ferrocenyl analogues of **9** and **10**, but they were remarkably unstable; the reason for this instability is unknown.

Satisfactory analytical and $^1H$ and $^{13}C$ NMR data

(11) Colbert, M. C. B.; Hodgson, D.; Lewis, J.; Long, N. J.; Raithby, P. R. *Polyhedron* **1995**, *14*, 2759.
(12) Kovar, R. F.; Rausch, M. D.; Rosenberg. H. *Organomet. Chem. Synth.* **1970/1971**, *1*, 173.

**Scheme 2**

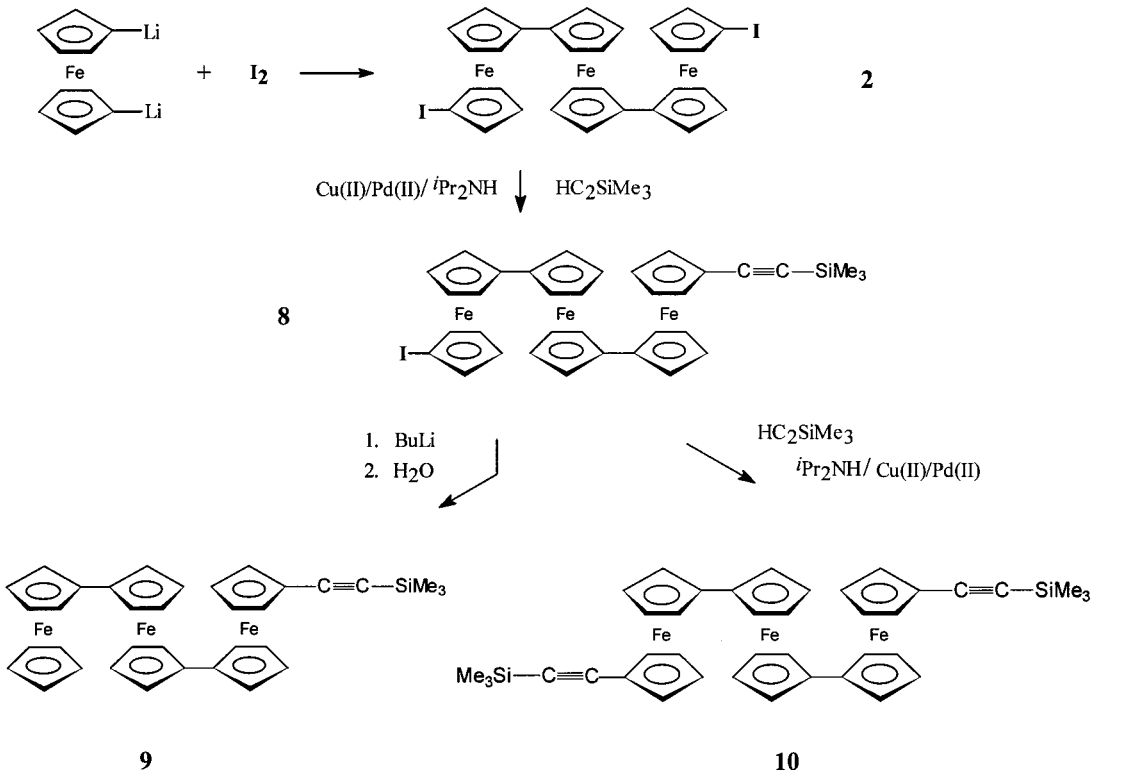


**Scheme 3**

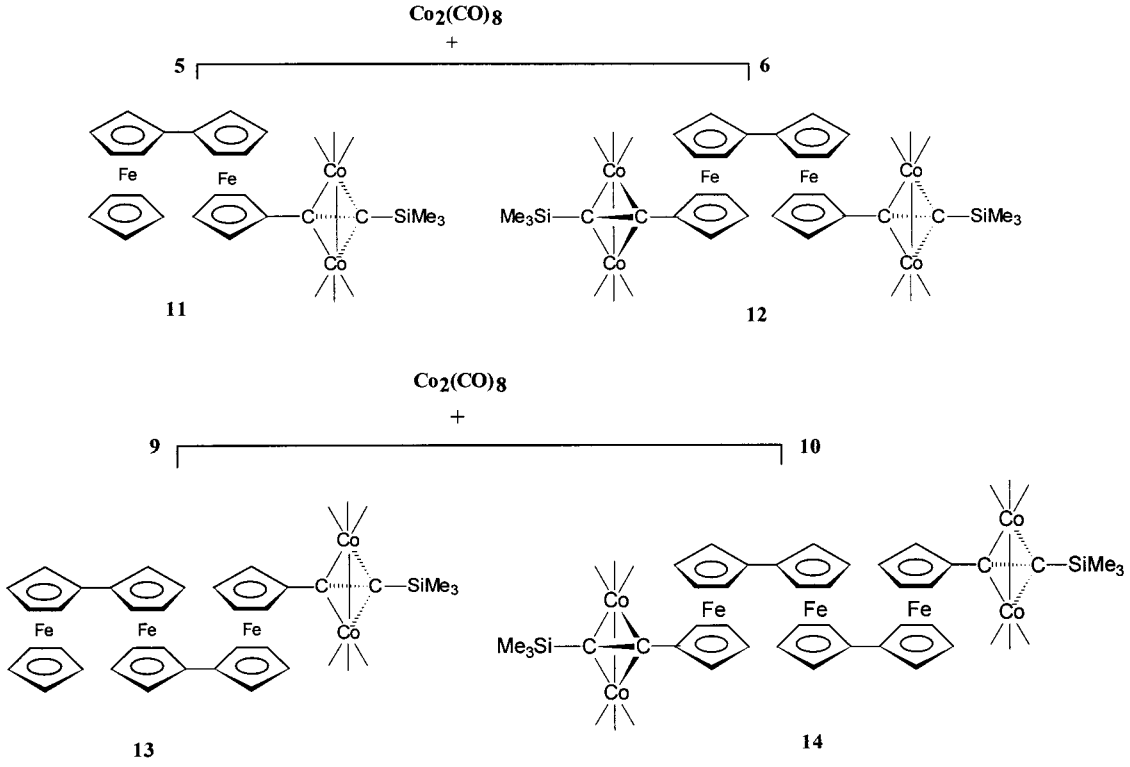


were obtained for **2**−**10**. The complicated NMR in the ferrocene region of the terferrocene complexes made assignment difficult, but the ratio of polyferrocene to trimethylsilyl resonances identified the products; this ratio was also useful in monitoring the reactions.

Reaction of **5, 6, 9**, or **10** with $Co_2(CO)_8$ gave the *green-black* $Co_2(CO)_6$ derivatives **11**−**14** (Scheme 3). Of note in the $^1$H NMR is the downfield shift of $\delta(SiMe_3)$ due to the deshielding effect of the metal fragment. The $\nu$(CO) bands were similar to those of other $Co_2(CO)_6$ complexes, the $A_1$ in-phase mode at 2083 cm$^{-1}$ indicating that there is no unusual steric congestion around the $Co_2(CO)_6$ unit caused by the polyferrocenyl moiety.[9]

Substitution reactions of the $Co_2(CO)_6$ complexes with dppm proceeded smoothly to give a series of *red-brown* $Co_2(CO)_4$dppm complexes **15**−**20** (Scheme 4).

**Scheme 4**

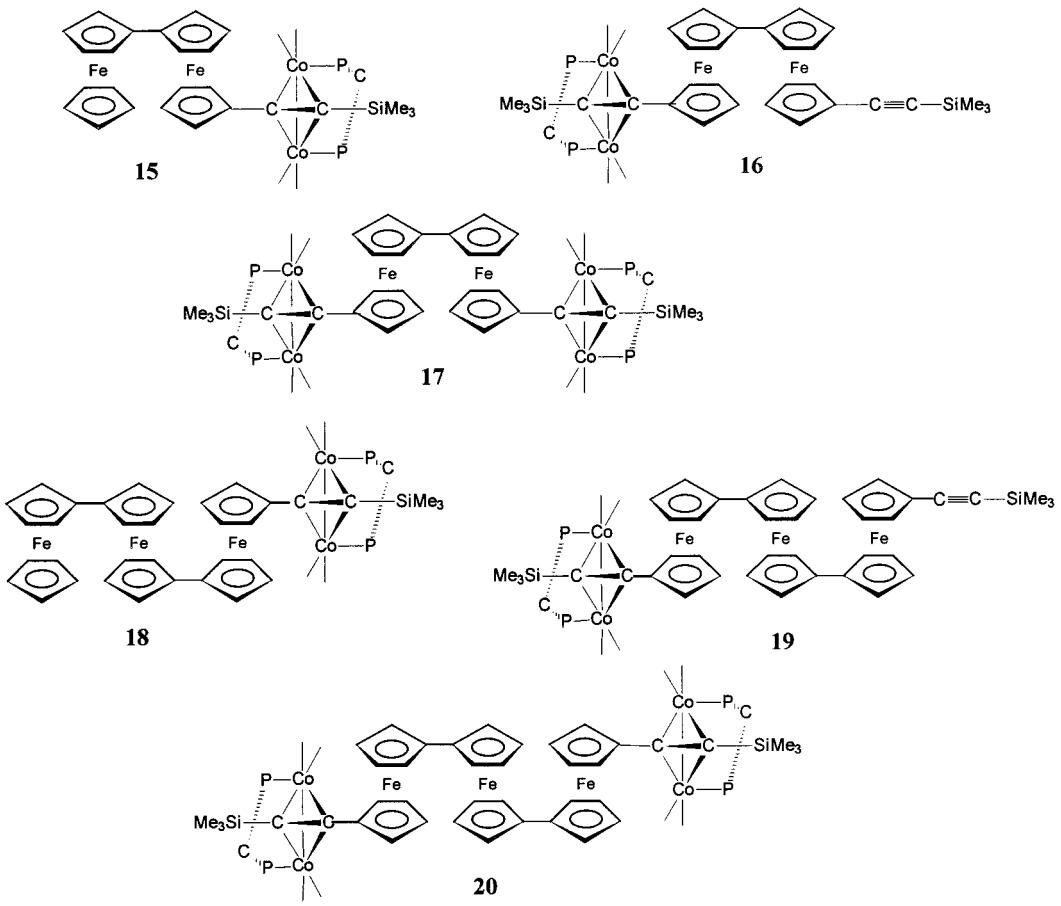




A change from green-black to red-brown color upon dppm coordination is unusual; in fact the reverse normally holds. A shift in $\nu$(CO) of ~60 cm$^{-1}$ to lower energy relative to the $Co_2(CO)_6$ complexes shows that the dppm has substituted symmetrically across the Co−Co bond.[9] The increase in electron density on the $Co_2(CO)_4$(alkyne) unit shifts $\delta_H(SiMe_3)$ further downfield to 0.55−0.56 ppm and clearly delineates the $SiMe_3$ groups in the complexes **16** and **19**, where there is one free C≡C group. Both **16** and **19** are produced in the reactions involving the bis-substituted $Co_2(CO)_6$ complexes **12** and **14**, respectively, with the metal fragment being lost during the reaction. This is a common feature for dppm reactions with polyalkyne−$Co_2(CO)_6$ complexes and is presumably because two $Co_2(CO)_4$dppm units cannot be accommodated sterically on two adjacent C≡C bonds.[9] A similar steric explanation could be advanced to account for the generic instability of **11**−**20** and the greater lability of the $Co_2(CO)_4$dppm compared to $Co_2(CO)_6$ analogues. An X-ray structural analysis of **17** was therefore undertaken in order to establish the steric parameters for these compounds.

**X-ray Structure Determination of 17.** The structure of compound **17** was determined by single-crystal X-ray structure analysis. A perspective view is shown in Figure 1, which defines the atom-numbering schemes. Selected bond length and angle information are given in Table 1. The unit cell contains discrete, well-separated molecules of the biferrocene complex and ethyl acetate solvent, with the closest intermolecular contact, not involving H atoms, being 3.214(2) Å between O(111) and C(3A).

Molecules of **17** consist of a biferrocene unit with approximately tetrahedral ($\mu$-alkyne)dicobalt moieties bound to the unsubstituted cyclopentadiene rings. They lie about an inversion center located at the midpoint of the C(8)−C(8a) bond of the fulvalenide ligand; this imposes a *trans*-conformation on the location of the ($\mu$-alkyne)dicobalt substituents with respect to the inversion center, with a steplike conformation[6a] of the two ferrocenyl rings. Both $Me_3SiC_2Co_2(CO)_4$(dppm) substituents point away from the central biferrocenyl unit and the outer C atoms of the alkyne groups each carry trimethylsilyl substituents. The cyclopentadiene rings in the biferrocene adopt an approximately staggered conformation, with a mean torsion angle C(m)−C(1g)−C(2g)−C(n) of 26.1(1)° (C(m) = C(3)−C(7), C(n) = C(8)−C(12), and C(1g) and C(2g) are the corresponding ring centroids), and the dihedral angle between the least-squares planes of the Cp rings of each ferrocenyl moiety is 3.59(25)°. The average Fe−C distances (2.049(8) Å) are not unusual, and the Fe atom is almost equidistant between the Cp ring (1.6502(9) Å) and fulvalenide (1.6546(9) Å). These are similar to the distances found in ferrocene itself.

The alkyne units adopt the normal *cis*-bent configuration, as expected for perpendicular acetylenes. The significant variation between the alkyne bend-back angles to the $Me_3Si$ substituent, Si(1)−C(1)−C(2) 148.15(15)°, and to the biferrocene, C(3)−C(2)−C(1) 140.86(17)°, undoubtedly reflects the requirement to minimize steric interactions between the ($\mu$-alkyne)dicobalt and biferrocenyl residues. The ($\mu$-alkyne)dicobalt cores of the $Me_3SiC_2Co_2(CO)_4$(dppm) moieties are typical of perpen-

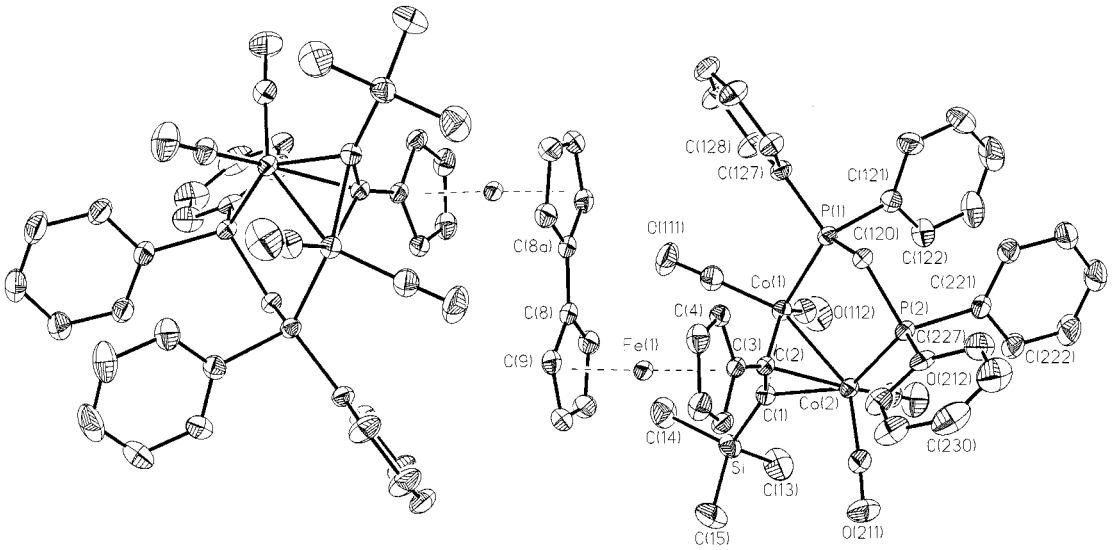


**Figure 1.** Perspective view of **17** showing the atom-numbering scheme, with displacement ellipsoids drawn at the 50% probablility level. For clarity H atoms have been omitted, and only two C atoms of consecutively numbered cyclopentadienyl and phenyl rings and the O atoms of the carbonyl ligands have been labeled.

**Table 1. Selected Bond Lengths (Å) and Angles (deg) for 17**

| | | | |
|---|---|---|---|
| Si−C(1) | 1.8425(19) | Co(1)−C(1) | 1.9828(18) |
| C(3)−C(2) | 1.458(2) | Co(1)−C(2) | 1.9658(18) |
| C(3)−C(4) | 1.437(2) | Co(2)−C(1) | 1.9812(18) |
| C(3)−C(7) | 1.438(2) | Co(2)−C(2) | 2.0073(17) |
| C(4)−C(5) | 1.421(3) | Co(1)−P(1) | 2.2139(5) |
| C(5)−C(6) | 1.419(3) | Co(1)−Co(2) | 2.4815(3) |
| C(6)−C(7) | 1.423(3) | Co(2)−P(2) | 2.2458(5) |
| C(8)−C(9) | 1.429(3) | P(1)−C(120) | 1.8411(18) |
| C(8)−C(12) | 1.430(3) | P(2)−C(120) | 1.8470(18) |
| C(8)−C(8)#1 | 1.472(4) | C(1)−C(2) | 1.353(3) |
| C(2)−C(1)−Si | 148.18(15) | C(1)−Co(2)−P(2) | 138.29(5) |
| C(1)−C(2)−C(3) | 140.86(17) | C(2)−Co(2)−P(2) | 100.11(5) |
| P(1)−Co(1)−Co(2) | 94.189(15) | | |
| P(2)−Co(2)−Co(1) | 98.560(15) | | |
| P(1)−C(120)−P(2) | 108.18(9) | | |

dicular alkyne complexes with an interline angle C(1)−C(2)/Co(1)−Co(2) of 91.5(1)°. The $C_2Co_2$ units are linked via a short, 1.458(2) Å, C−C single bond to the cyclopentadiene rings of the biferrocene. This bond distance suggests some degree of electron delocalization between the alkyne and biferrocene units (vide infra). The alkyne C(1)−C(2) bond length, 1.353(3) Å, is in reasonable agreement with those found in other $C_2Co_2$ systems. However, distortion of the quasi tetrahedral $C_2Co_2$ core is evidenced by the nonequivalence of the Co−C bond lengths [Co(1)−C(1) 1.9828(18) Å, Co(1)−C(2) 1.9658(18) Å, Co(2)−C(1) 1.9812(18) Å, Co(2)−C(2) 2.0073(17) Å]; the net effect tilts the C(1)−C(2) vector relative to the Co−Co bond toward the central biferrocenyl moiety. The Co(1)−Co(2) bond is long, 2.4815(3) Å, in comparison with most ($\mu$-alkyne)dicobalt complexes with ($\mu$-$\eta^2$)-bound dppm ligands. In such compounds Co−Co bond distances are generally in the range 2.46−2.47 Å; indeed that is also the norm for unsubstituted $C_2Co_2(CO)_6$ systems.[19] Co−Co bonds as long as 2.50−2.52 Å are found where two P donor atoms chelate to a single Co atom or when a second dppm or dam[18a] ligand binds in ($\mu$-$\eta^2$)-fashion across the Co−Co bond. Co−Co bond extension in these cases has been attributed to steric affects, and the lengthening observed here is most likely a response by the molecule to the significant steric requirements of the biferrocenyl moiety and the adjacent dppm ligands.

The dppm ligands adopt ($\mu$-$\eta^2$) coordination, bridging the Co−Co bonds of the $C_2Co_2$ fragment. Each cobalt atom also carries an "axial" CO and "pseudoequatorial" CO and P ligands. The CO and P atoms deviate only slightly from the classical "sawhorse" arrangement with respect to the cobalt atoms (torsion angles P(1)−Co(1)−Co(2)−P(2) 6.19(2)°; C(111)−Co(1)−Co(2)−C(211) 17.6(2)°; (112)−Co(1)−Co(2)−C(212) 7.6(1)°). The Co−P bond distances are unremarkable and the bridging dppm ligands bind so as to minimize steric interactions between the phenyl rings of the dppm ligands and the adjacent ferrocenyl centers.

**Redox Chemistry.** The molecules described herein provided an opportunity to explore the efficiency of intravalence charge transfer within the polyferrocene core when alkyne ferrocenyl groups are attached and, in the $Co_2(CO)_4$dppm complexes, where the communication axis is no longer linear.

**Electrochemistry of 5, 6, 9, and 10.** These complexes display the typical one-electron, chemically reversible, oxidation waves of the ferrocenyl units in the cyclic and square wave voltammetry. The number of ferrocenyl units determines the number of *i*/*V* responses. For example, **10** with three units displays three discrete waves (Figure 2). Ferrocene is a net electron donor, and as a consequence the potential for the first oxidation process $E_{1/2}^{+/0}$ moves cathodically as the number of ferrocenyl rings in the polyferrocene $Fc(Fc)_N$ ($N = 1-3$)



(13) Barlow, S.; O'Hare, D. *Chem. Rev.* **1997**, *96*, 637.
(14) Seiler, P.; Dunitz, J. D. *Acta Crystallogr. Sect. B* **1979**, *35*, 1068.
(15) Bonnet, J.-J.; Mathieu, R. *Inorg. Chem.* **1978**, *17*, 1973.
(16) Hoffman, D. M.; Hoffmann, R.; Fisel, C. R.. *J. Am. Chem. Soc.* **1982**, *104*, 3858.
(17) Dickson R. S.; Fraser, P. J. *Adv. Organomet. Chem.* **1974**, *12*, 323.
(18) (a) Bird, P. H.; Fraser A. R.; Hall, D. N. *Inorg. Chem.* **1977**, *16*, 1023. (b) Lewis, J.; Lin, B.; Khan, M. S.; Al-Mandhary, M. R. A.; Raithby, P. R. *J. Organomet. Chem.* **1994**, *484*, 161. McAdam, C. J.; Duffy, N. W.; Robinson, B. H.; Simpson, J. *Organometallics* **1996**, *15*, 3935.
(19) Bianchini, C.; Dapporto, P.; Meli, A. *J. Organomet. Chem.* **1979**, *174*, 205.

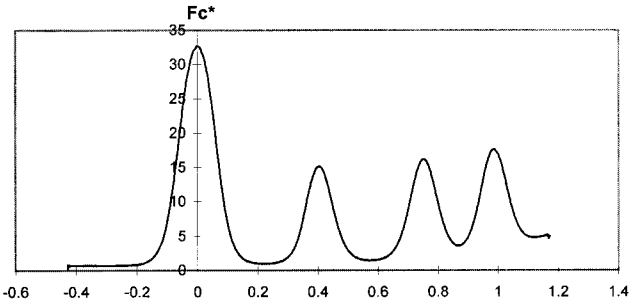


**Figure 2.** Square wave voltammogram (60 Hz, 2 mV) of **10** in $CH_2Cl_2$, Pt, 0.1 $^nBu_4NPF_6$.

**Table 2. Electrochemical Data**

| | $[E_{1/2}]^{a,b}$ | | | | | | |
|---|---|---|---|---|---|---|---|
| | $[1^+/0]$ | $[2^+/1^+]$ | $[3^+/2^+]$ | $[4^+/3^+]$ | $\Delta E(1)^c$ | $\Delta E(2)^c$ | $\Delta E(3)^{b,c}$ |
| $Fc_2$ | 0.46 | 0.80 | | | 340 | | |
| **5** | 0.50 | 0.81 | | | 310 | | |
| **6** | 0.51 | 0.81 | | | 300 | | |
| **7** | 0.43 | 0.57 | 0.62 | 0.97 | 350 | | *140* |
| **21a**[d] | 0.54 | 0.90 | | | 360 | | |
| **21b**[d] | 0.50 | 0.95 | | | 450 | | |
| **15** | 0.46 | 0.76 | *1.11* | | 300 | | |
| **17** | 0.48 | 0.66 | *1.02* | *1.26* | 180 | 360 | *240* |
| $Fc_3$[f] | 0.37 | 0.59 | 0.97 | | 220 | 380 | |
| **9** | 0.42 | 0.73 | 0.99 | | 310 | 260 | |
| **10** | 0.41 | 0.76 | 0.99 | | 350 | 230 | |
| **18** | 0.37 | 0.55 | 0.85 | *1.05* | 180 | 300 | *200* |
| **20** | 0.36 | 0.51 | 0.70 | *1.06*[e] | 150 | 190 | *40*[e] |
| $Fc_4$[f] | 0.31 | 0.51 | 0.76 | 1.04 | 200 | 250 | 280 |
| $FcC_2SiMe_3$ | 0.61 | | | | | | |
| $FcC_2Fc$ | 0.63 | 0.76 | | | 130 | | |

[a] Volts; all data referenced to decamethylferrocene; Pt, 200 mV $s^{-1}$ in dichloromethane. [b] Data in italics refer to $Co_2$ redox center. [c] In mV. [d] Compounds **21a** and **21b**, $Fc_2(C{\equiv}CPh)_2$ and $Fc_2(C{\equiv}CH)_2$, respectively.[23] [e] Two-electron process in CV; 40 mV estimated from SQV. [f] Ref 4a.

increases (Table 2). The relationship, in dichloromethane at 200 mV $s^{-1}$ referenced against decamethylferrocene, can be expressed as $E_{1/2}{}^{+/0}(V) = [0.55 - N(0.09)]$. A pendant $-C{\equiv}C-SiMe_3$ on a ferrocenyl redox unit causes an anodic shift in $E_{1/2}{}^{+/0}$ (Table 2), and for **5** and **9** the relationship is $E_{1/2}{}^{+/0}(V) = [0.55 - N(0.09) + 0.05]$. Intuitively, the $-C{\equiv}C-SiMe_3$ functional group should not withdraw electron density from the ferrocenyl moiety, and it is probable that the anodic shift is a reflection of the relative stability of the mixed-valence $Fc-Fc_N{}^+$ cations. In support of a noninductive explanation is the fact that the addition of a second $-C{\equiv}C-SiMe_3$ to the polyferrocenyl core has virtually no effect on $E_{1/2}{}^{+/0}$ (cf. compare **5** and **6**, **9** and **10**).

For the polyferrocenes $\Delta E_{1/2}(1)$, the separation between $E_{1/2}{}^{+/0}$ and $E_{1/2}{}^{2+/+}$, decreases with increasing size of the ferrocenyl core. It is noteworthy that $\Delta E_{1/2}(1) < Fc(Fc)_N\ \Delta E_{1/2}(2)$ for $N = 2$ and 3, presumably because the higher charge is effectively dispersed in the polyferrocene, thereby stabilizing the cations. Given the $C_2$-$SiMe_3$ substituent effect noted above, it was therefore surprising to find that, first, $\Delta E_{1/2}(1)$ is essentially the same for the comparable bi- and terferrocenes **5**/**9** and **6**/**10** and, second, the reverse order $\Delta E_{1/2}(1) > \Delta E_{1/2}(2)$ for **9** and **10**. Thus $\Delta E_{1/2}(1)$, the separation between $E_{1/2}{}^{+/0}$ and $E_{1/2}{}^{2+/+}$, for **6** is 300 mV, whereas the sequential values for **10** are $\Delta E_{1/2}(1) = 350$ mV and $\Delta E_{1/2}(2) = 230$ mV at 200 mV $s^{-1}$. An explanation for the variation in the $\Delta E_{1/2}$ values is likely to lie in the different charge separations in the oxidized species, but there is no satisfactory theoretical model at present.

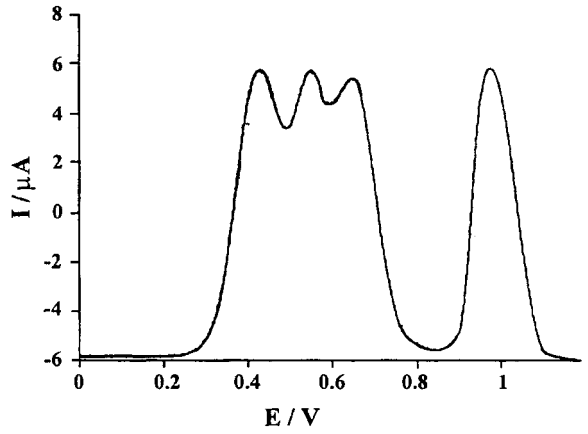


**Figure 3.** Square wave voltammogram (60 Hz, 2 mV) of **7** in $CH_2Cl_2$, Pt, 0.1 $^nBu_4NPF_6$.

**Scheme 5**

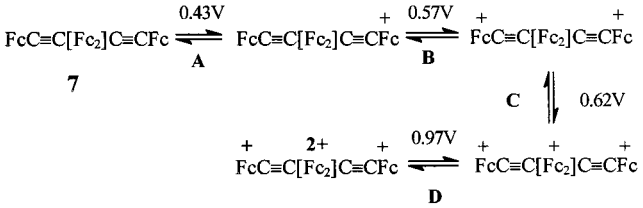


**Electrochemistry of 7.** Compound **7**, which has four ferrocenyl units, displayed four reversible one-electron oxidation processes in its cyclic and square wave voltammetry (Figure 3). Although the four Fc units could be grouped as an "inner" biferrocenyl core and two Fc termini there, is no reason a priori why all four should not communicate. Data for the sequence $Fc(C{\equiv}C)_nFc$[22] and $Fc_2(C{\equiv}CPh)_2$[23] show that the interpolation of an alkyne between Fc termini or attachment of an alkyne link to $Fc_2$ causes an anodic shift in $E_{1/2}{}^{+/0}$. On the other hand, a $Fc_2$ group would act as a good donor to the Fc termini. For these reasons $E_{1/2}{}^{+/0}$ (**A**) at 0.43 V is assigned to oxidation of the two communicating Fc termini. It is unlikely that $\Delta E_{1/2}$ between the "outer" Fc in **7** would be much greater than that for FcC≡CFc (130 mV). $E_{1/2}{}^{2+/+}$ (**B**) at 0.57 V [$\Delta E_{1/2}(I) = 140$ mV] is therefore assigned to the second oxidation process of the Fc termini (Scheme 5). The remaining two oxidation processes at $E_{1/2} = 0.62$ V (**C**) and 0.97V (**D**) are assigned to the $Fc_2$ core; as expected, these are anodic of those for **6** since there is a positive charge on the ferrocenyl termini. Support for this assignment comes from the consistency of the "communication parameter" of ~300 mV for the $Fc_2$ core in **5**−**7**.

The important conclusions from these data are the following: the interpolation of a $Fc_2$ unit *does not impede the communication* between the Fc termini, and, to a first approximation, *communication* between the "outer" and "inner" sets of Fc redox centers is mutually exclusive.

(20) Aggarwal, R. P.; Connelly, N. G.; Crespo, M. C.; Dunne, B. J.; Hopkins, P. M.; Orpen, A. G. *J. Chem. Soc., Dalton Trans.* **1992**, 655.

(21) Gregson, D.; Howard, J. A. K. *Acta Crystallogr.* **1983**, *C39*, 1024

(22) Ribot, A.-C.; Launay, J. P.; Sachtleben, M. L.; Li, H., Spangler, C. W. *Inorg. Chem.* **1996**, *35*, 3735.

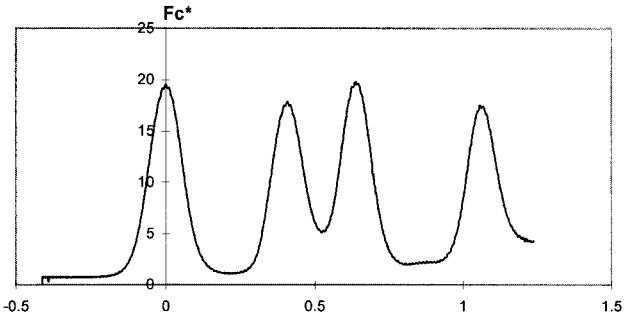


**Figure 4.** Square wave voltammogram (60 Hz, 2 mV) of **15** in $CH_2Cl_2$, Pt, 0.1 $^nBu_4NPF_6$.

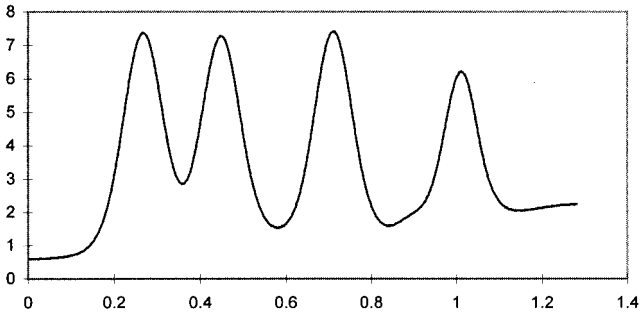


**Figure 5.** Square wave voltammogram (60 Hz, 2 mV) of **18** in $CH_2Cl_2$, Pt, 0.1 $^nBu_4NPF_6$.

**Electrochemistry of $Co_2(CO)_4$dppm Derivatives.** Because of the instability of the $Co_2(CO)_6$ derivatives and the rapid ECE reactions involving the carbonyl fragment,[8,10] a detailed examination of the oxidation electrochemistry of only the $Co_2(CO)_4$dppm derivatives was carried out. The latter complexes also provided an opportunity to examine whether a disparate redox center also behaved independently of the polyferrocenyl core.

The effect on the −C≡C− bond by coordination and electron donation from the $Co_2(CO)_4$dppm unit caused a small cathodic shift in the polyferrocenyl core potentials compared with the parent alkynes (Table 2). The $Fc_2$ complex with one $Co_2(CO)_4$dppm unit **15** displayed cyclic and square wave voltammetric responses which clearly delineate the redox centers (Figure 4). Two chemically reversible one-electron processes $E_{1/2} = 0.46$ and 0.76 V are assigned to the $Fc_2$ core and the chemically reversible one-electron step at more positive potentials, $E_{1/2} = 1.11$ V, to the $Co_2(CO)_4$dppm unit. It is significant that $\Delta E_{1/2}$[$Fc_2$] for **15** is identical to that of its parent **5**, indicating that perturbation of the −C≡C− does not affect communication within the $Fc_2$ core, the mutual exclusivity noted above. Furthermore, $E_{1/2}$ for the oxidation of the $Co_2(CO)_4$dppm unit in **15** is the same as that in Fc[$C_2Co_2(CO)_4$dppm]$C_2$Fc,[9a] illustrating that the Coulombic effect of two positively charged Fc moieties is equivalent whether they are at the terminus or as a biferrocene unit.

**Scheme 7**

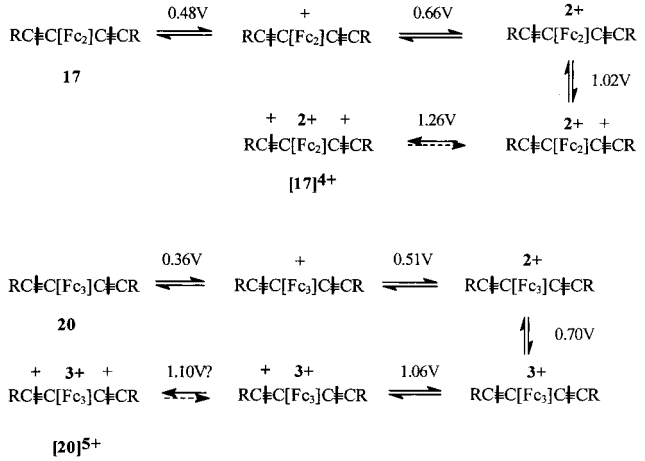


The situation is different for the $Fc_3$ complex **18**. Four reversible one-electron processes are displayed in the cyclic and square wave voltammetry of **18** (Figure 5); the first three have $E_{1/2}$ values similar to those for **10** and are assigned to the $Fc_3$ core; that at $E_{1/2} = 1.06$ V is assigned to a chemically reversible oxidation of the $Co_2(CO)_4$dppm unit (Scheme 6). Coordination of the cluster to the alkyne link has reduced $\Delta E(1)$ from 310 (cf. **9**) to 180 mV but with little change in $\Delta E(2)$. This is in contrast with the $Fc_2$ system, where there was little perturbation of the intra-metallocene "communication" by coordinating the cluster unit.

The bis-substituted complexes **17** and **20** gave the opportunity to investigate the interaction between two $Co_2(CO)_4$dppm units modulated by an $Fc_N$ core. Assignments for these complexes are given in Scheme 7. For the $Fc_2$ complex **17** the core $Fc_2$ and $Co_2(CO)_4$dppm potentials are little changed from **15**, and extensive communication is retained between the $Co_2(CO)_4$dppm clusters ($\Delta E_{1/2} = 240$ mV). As a consequence, four one-electron waves are seen in the voltammetry of **17** (Figure 6). Those associated with the $Fc_2$ core are chemically reversible, whereas the cluster oxidation processes are reversible at fast scan rates (>1 V $s^{-1}$). In contrast, **20** displays three reversible one-electron responses due to the $Fc_3$ core and a *two*-electron response in the cyclic voltammogram (Figure 7); a small resolution ($\Delta E \approx 40$mV) of the two-electron response is just discernible in the square wave voltammogram. The two-electron $Co_2(CO)_4$dppm oxidation process is chemically reversible only at low temperatures and fast scan rates. It is interesting that for these bis complexes the collapse of the linear alkyne link by coordination of two

**Scheme 6**

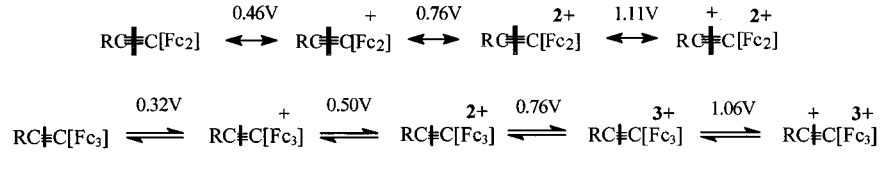

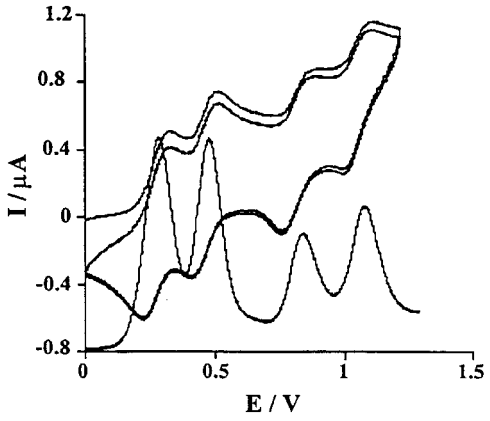


**Figure 6.** Cyclic voltammogram of **17** in $CH_2Cl_2$, Pt, 0.1 $^nBu_4NPF_6$, 100 mV $s^{-1}$.

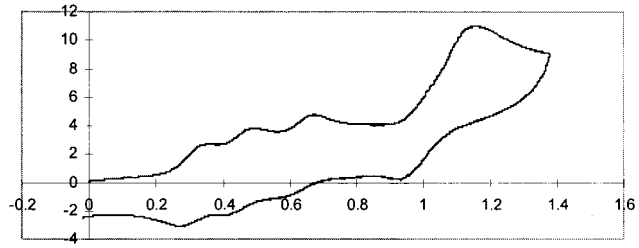


**Figure 7.** Cyclic voltammogram and square wave voltammogram (60 Hz, 2 mV) of **20** in $CH_2Cl_2$, Pt, 0.1 $^nBu_4NPF_6$, 200 mV $s^{-1}$.

$Co_2(CO)_4$dppm units reduces communication both within the $Fc_N$ core and between the two $Co_2(CO)_4$dppm redox centers.

Despite the apparent longevity of the oxidized species of **6**−**20** at the electrode surface on the electrochemical time scale, no mixed valence species could be isolated. Controlled electrochemical oxidation in an OTTLE cell and chemical oxidation produced color changes and shifts in the UV/visible/IR spectra, but the species produced were very unstable. Bulk oxidation invariably led to decomposition.

## Conclusion

These studies show that ethynylpolyferrocenyl units can function as effective modular links in the construction of molecular switches and arrays. The controlled synthesis of the diiodopolyferrocenes provides synthons which, via standard coupling methods, can be used to incorporate the polyferrocene core into linear or polyhedral arrays. An increase in the lability of the molecules as the polyferrocene backbone expands does limit this route. For reasons that are not understood this was especially evident when ferrocenyl groups occupied the terminal positions and $Fc_3$-ethynylferrocene compounds could not be characterized. Nevertheless, it has been found that a series of molecules in which the biferrocene is linked to fluorophores have reasonable stability.[23] The observation that each redox center, whether a ferrocenyl terminus, a $Co_2(CO)_4$dppm unit, or the polyferrocenyl core, can act almost independently of each other while still being subject to inductive influences is significant. While the $Fc_2$ core did not modulate the redox chemistry of the terminal groups, the $Fc_3$ core did reduce the interaction between the pendant redox centers. To design a molecular array with predetermined tunable electron transfer characteristics, it will be necessary to have a better description of what is meant by "communication" in these systems. That is, a description of the orbital energies for the various mixed valence species in an oxidation sequence. However, at the present time we have no theoretical model that can predict the subtle trends that have been noted in this work. It is doubtful that the $\Delta E$ parameters derived for the $Fc_2$ and $Fc_3$ molecules give other than a crude qualitative measure of "communication".

(23) Duffy, N. W. Ph.D. Thesis, University of Otago, 1997; work in progress.

## Experimental Section

All reactions were carried out under anerobic conditions using distilled and dried solvents. Transfers involving lithium reagents were carried out using a cannula. $Fc_2I_2$ (**1**) was prepared by the literature method.[12] Microanalyses were carried out by the Campbell Microanalytical Laboratory, University of Otago. The FAB mass spectra were recorded on a Kratos MS80RFA instrument with an Iontech ZN11NF atom gun. Solvents were dried and distilled by standard procedures. Infrared spectra were recorded on a Digilab FX60 spectrometer. $^1$H NMR were recorded on a Gemini 200 MHz spectrometer and the $^{31}$P NMR on a Varian VXR 300 MHz spectrometer. Voltametric responses were recorded in dichloromethane on an EG & G PAR 273 electrochemical analyzer interfaced to a microcomputer using PAR M270 software with the solution in a three-electrode cell. Potentials were referenced with decamethylferrocene as an internal reference (ferrocene = 0.55 V in $CH_2Cl_2$).

**Preparation of 3, 5, and 6.** To a stirred solution of **1** (293 mg, (0.47 mmol) in diisopropylamine (25 mL) at 20 °C was added trimethylsilylacetylene (0.13 mL, 0.92 mmol) followed by 2 mol % $Cu(OAc)_2/(PPh_3)_2PdCl_2$. The reaction mixture was refluxed for 30 min and solvent stripped in vacuo. The products were separated on preparative silica gel plates in hexane/dichloromethane (4:1) to give **3** (band 2) as a dark red solid (83 mg, 25%). Anal. Calcd for $C_{25}H_{25}Fe_2ISi$: C, 50.71; H, 4.26. Found: C, 50.88; H, 4.22. Mass spectrum: *m/e* 592 ($M^+$). $^1$H NMR ($CDCl_3$) $\delta$: 0.25 (s, 9H, $-SiMe_3$), 3.9−4.4 (m, 16H, $Fc_2$-*H*). **3** (117 mg, 0.20 mmol) was dissolved in dry tetrahydrofuran and cooled to −78 °C. *n*-Butyllithium (0.2 mL) was then added and the mixture stirred for 1 h, after which it was warmed to room temperature. Water was added and the mixture was left to stir for a further 10 min. The reaction mixture was extracted into hexane and recrystallized from hexane/dichloromethane to give 72 mg (75%) of **5** as dark orange microcrystals. Anal. Calcd for $C_{25}H_{26}Fe_2Si$: C, 64.4; H, 5.62. Found: C, 64.09; H, 5.57. Mass spectrum: *m/e* 466 ($M^+$). $^1$H NMR ($CDCl_3$) $\delta$: 0.24 (s, 9H, $-SiMe_3$), 4.0−4.4 (m, 17H, $Fc_2$-*H*). Trimethylsilyl acetylene (0.17 mL) was coupled to **3** (372 mg, 0.6 mmol) using 2 mol % $Cu(OAc)_2/(PPh_3)_2PdCl_2$. The reaction mixture was separated on $SiO_2$ plates in hexane/dichloromethane (4:1) to yield 76 mg (23%) of **6** (this compound has been prepared directly from **1**).[11] Anal. Calcd for $C_{30}H_{34}Fe_2Si_2$: C, 64.06; H, 6.09. Found: C, 63.89; H, 6.21. Mass spectrum (FAB): *m/e* 562 ($M^+$). $^1$H NMR ($CDCl_3$) $\delta$: 0.23 (s, 18H, $-SiMe_3$), 4.01 (4H, t, Fc $\beta H$), 4.18 (4H, t, Fc $\alpha H$), 4.21 (4H, t, Fc $\beta' H$), 4.37 (4H, t, Fc $\alpha' H$).

**Preparation of 4 and 7.** A stirred solution of **1** (293 mg, 0.23 mmol), ethynyl ferrocene (120 mg, 0.57 mmol), and 2 mol % $Cu(OAc)_2/(PPh_3)_2PdCl_2$ in diisopropylamine (25 mL) was refluxed for 15 min. The solvent was stripped in vacuo. The products were separated on preparative silica gel plates in hexane/dichloromethane (4:1). Bands 1 and 2 gave unreacted **1** and diferrocenyl butadiyne, respectively. Band 3 gave **4**; FAB-MS: *m/e* 704 ($M^+$). Band 4 was identified as **7**, a dark

red solid, (23 mg, 13%). Anal. Calcd for $C_{44}H_{34}Fe_4$: C, 67.23; H, 4.33. Found: C, 66.89; H, 4.21. Mass spectrum (EI): *m/e* 786 ($M^+$). $^1$H NMR ($CDCl_3$) $\delta$: 4.06 (4H, t, Fc $\beta H$), 4.20 (4H, t, Fc $\beta' H$), 4.22 (4H, t, Fc $\alpha H$), 4.23 (s, 10H, $C_5H_5$), 4.27 (4H, t, Fc $\beta'' H$), 4.43 (4H, t, Fc $\alpha' H$), 4.44 (4H, t, Fc $\alpha'' H$).

**Preparation of 2.** To ferrocene (5.6 g) in hexane (170 mL) was added n-BuLi (40 mL) and TMEDA (10 mL). Iodine (7 g) in THF (80 mL) was then added with vigorous stirring to the solution containing the precipitated dilithioferrocene−TMEDA complex, and the reaction mixture was stirred for 1 h, then refluxed for 30 min. The mixture was extracted into dichloromethane, and the organic layer washed with water and then dried over magnesium sulfate. Separation of the iodo polyferrocene derivatives was achieved by column chromatography on alumina. Hexane eluent was progressively enriched with $CH_2Cl_2$ to remove mono- and biferrocenes. The desired product was eluted next by ethyl acetate to give **2** as an orange powder (2.05 g, 24%). Anal. Calcd for $C_{30}H_{24}Fe_3I_2$: C, 44.71; H, 3.00. Found: C, 44.88; H, 2.94. FAB-MS: *m/e* 806 ($M^+$), 680 ($M - I^+$). $^1$H NMR ($CDCl_3$) $\delta$: 3.91, 4.06, 4.10 {3 × (t, 4H, $Fc_3$-*H*)}, 4.15 (m, 12H, $Fc_3$-*H*).

**Preparation of 8 and 10.** To a stirred solution of **2** (480 mg, 0.6 mmol) in diisopropylamine (50 mL) was added trimethylsilylacetylene (0.34 mL) followed by 2 mol % $Cu(OAc)_2$/$(PPh_3)_2PdCl_2$, and the solution was refluxed for 3 h. The solvent was stripped in vacuo and the residue separated on preparative silica gel plates, eluting with hexane/dichloromethane (10:1), to give **8** (50 mg, 11%) as a very unstable brown solid. FAB-MS: *m/e* 776 ($M^+$). $\delta_H$ ($CDCl_3$): 0.23 (s, 9H, $-SiMe_3$), 3.9−4.2 (m, 24H, $Fc_3$-*H*)}; the compound gave a positive Beilstein test. Recrystallization of the next band from dichloromethane/hexane gave **10** as needlelike orange crystals (100 mg, 22%). Anal. Calcd for $C_{40}H_{42}Fe_3Si_2$: C, 64.35; H, 5.67. Found: C, 64.15; H, 5.50. FAB-MS: *m/e* 746 ($M^+$). $^1$H NMR ($CDCl_3$) $\delta$: 0.22 (s, 18H, $-SiMe_3$); 3.96, 4.05, 4.13 {3 × (t, 4H, $Fc_3$-*H*)}, 4.17 (m, 12H, $Fc_3$-*H*).

**Preparation of 9.** The iodide **8** (80 mg) was dissolved in THF and cooled to −78 °C, n-BuLi (hexane, 0.5 mL) was added, and the reaction mixture was stirred for 1 h before being brought to room temperature. Water was added and the reaction mixture stirred for a further 15 min. The organic layer was collected and the solvent stripped in vacuo. The *residue* was dissolved in hexane, washed with water, dried over magnesium sulfate, and recrystallized from dichloromethane/hexane to give dark red **9** (41 mg). Anal. Calcd for $C_{35}H_{34}Fe_3Si$: C, 64.64; H, 5.27. Found: C, 64.66; H, 5.40. FAB-MS: *m/e* 650 ($M^+$). $^1$H NMR ($CDCl_3$) $\delta$: 0.22 (s, 9H, $-SiMe_3$), 3.9−4.3 (m, 25H, $-Fc_3H$).

**Preparation of 11−14.** Dicobaltoctacarbonyl (510 mg, 1.5 mmol) was added to **5** (443 mg, 0.95 mmol) in hexane/dichloromethane (1:1) and the reaction mixture stirred at ambient temperature for 2 h. The solvent was removed and the resulting mixture separated by chromatography on silica gel preparative plates in hexane/dichloromethane (5:1). The green band was removed and crystallized from hexane to give green-black crystals of **11** (102 mg 14%). Anal. Calcd for $C_{31}H_{26}Co_2Fe_2O_6Si$: C, 49.5; H, 3.48. Found: C,49.56; H, 3.35. $^1$H NMR ($CDCl_3$) $\delta$: 0.43 (s, 9H, $-SiMe_3$), 3.9−4.4 (m, 17H, $Fc_2$-*H*). IR $\nu_{CO}$ (hexane): 2083, 2046, 2021, 2013, 2002 $cm^{-1}$.

The following complexes were prepared by a similar procedure. **12:** Compound **6** (224 mg, 0.4 mmol) and an excess of dicobalt octacarbonyl gave 181 mg (40%) of green crystalline **12**. Anal. Calcd for $C_{42}H_{34}Co_4Fe_2O_{12}Si_2$: C, 44.47; H, 3.02. Found: C, 44.48; H, 3.30. FAB-MS: *m/e* 1134 ($M^+$), sequence 1050−798 ($M^+ - 3CO...M^+ - 12CO$). $^1$H NMR ($CDCl_3$) $\delta$: 0.44 (s, 18H, $-SiMe_3$), 4.0−4.4 (m, 16H, $Fc_2$-*H*). IR $\nu_{CO}$ (hexane): 2083, 2046, 2022, 2014, 2003 $cm^{-1}$. **13:** Compound **9** (153 mg, 0.235 mmol) and dicobalt octacarbonyl (200 mg, 0.59 mmol) gave 72 mg (33%) of green-black crystalline **13**. Anal. Calcd for $C_{41}H_{34}Co_2Fe_3O_6Si$: C, 52.60; H, 3.66. Found: C, 52.83; H, 3.63. FAB-MS: *m/e* 936 ($M^+$), sequence 852−600 ($M^+ - 3CO...M^+ - 6CO$). $^1$H NMR ($CDCl_3$) $\delta$: 0.43 (s, 9H, $-SiMe_3$), 3.9−4.3 (m, 25H, $Fc_3$-*H*). IR $\nu_{CO}$ (hexane): 2083, 2045, 2021, 2013, 2002 $cm^{-1}$. **14:** Compound **10** (100 mg, 0.15 mmol) and dicobalt octacarbonyl (206 mg, 0.6 mmol) gave 78 mg (44%) of green-black crystalline **14**. Anal. Calcd for $C_{52}H_{42}Co_4Fe_3O_{12}Si_2$: C, 47.37; H, 3.21. Found: C, 47.85; H, 3.32. FAB-MS: *m/e* 1318 ($M^+$), sequence 1234−982 ($M^+ - 3CO...M^+ - 12CO$). $^1$H NMR ($CDCl_3$) $\delta$: 0.43 (s, 18H, $-SiMe_3$), 4.0−4.3 (m, 24H, $Fc_3$-*H*). IR $\nu_{CO}$ (hexane): 2082, 2045, 2021, 2013, 2002 $cm^{-1}$.

**Table 3. Crystal Data and Structure Refinement for 17**

| | |
|---|---|
| empirical formula | $C_{96}H_{94}Co_4Fe_2O_{12}P_4Si_2$ |
| molecular formula | $C_{88}H_{78}O_8Si_2P_4Fe_2Co_4$, $2(C_4H_8O_2)$ |
| fw | 1967.19 |
| cryst syst | monoclinic |
| space group | *P*2(1)/*c* |
| abs coeff | 1.167 $mm^{-1}$ |
| final *R* indices [$I>2\sigma(I)$] | R1 = 0.0295, wR2 = 0.0796 |
| (all data) | R1 = 0.0361, wR2 = 0.0871 |
| goodness-of-fit on $F^2$ | 1.131 |
| temperature | 203(2) K |
| wavelength | 0.71073 Å |
| unit cell dimens | $a$ = 11.9329(2) Å |
| | $b$ = 25.7059(6) Å |
| | $c$ = 15.7314(2) Å |
| | $\beta$ = 107.71(1)° |
| volume | 4596.72(14) $Å^3$ |
| *Z* | 2 |
| density (calcd) | 1.421 $Mg/m^3$ |
| *F*(000) | 2028 |
| no. of reflns collected | 10 324 |
| no. of ind reflns | 10 324 [*R*(int) = 0.0000] |

**15−20.** A solution of **12** (137 mg, 0.12 mmol) and excess bis(diphenylphosphino)methane in benzene (25 mL) was heated under reflux for 20 min. The solvent was stripped, and the products were separated on preparative silica gel plates, eluting with ether/hexane (1:1). Removal of the first red band gave **16**, 83 mg as a red-brown solid. FAB-MS: *m/e* 1176 ($M^+$). $^1$H NMR ($CDCl_3$) $\delta$: 0.22 (s, 9H, $-C\equiv C-SiMe_3$), 0.56 (s, 9H, −cluster$-SiMe_3$), 3.2−3.6 (m, 2H, $-CH_2-$), 3.9−4.4 (m, 16H, $Fc_2$-*H*), 6.9−7.3 (m, 20H, Ph-*H*). $\delta_P$ ($CDCl_3$): 34 (s). IR $\nu_{CO}$ (hexane): 2017, 1991, 1965, 1950 $cm^{-1}$; $\nu_{C\equiv C}$: 2148 $cm^{-1}$. From the same reaction removal of the second red band from plate chromatography gave 99 mg of red-brown crystalline **17**. Anal. Calcd for $C_{88}H_{78}Co_4Fe_2O_8P_4Si_2$: C, 59.01; H, 4.39. Found: C, 58.81; H, 4.72. $^1$H NMR ($CDCl_3$) $\delta$: 0.56 (s, 18H, $-SiMe_3$), 3.2−3.6 (m, 2H, $-CH_2^-$), 3.9−4.4 (m, 16H, $Fc_2$-*H*), 6.9−7.3 (m, 40H, Ph-*H*). $\delta_P$ ($CDCl_3$): 34 (s). IR $\nu_{CO}$ (hexane): 2018, 1992, 1965, 1950, 1926 $cm^{-1}$.

By a similar procedure. **15:** From **11**, with ethyl acetate/hexane (1:5), gave red-brown **15** (37%). Anal. Calcd For $C_{54}H_{48}Co_2Fe_2O_4P_2Si$: C, 60.02; H, 4.48. Found: C, 60.29; H, 4.86. $^1$H NMR ($CDCl_3$) $\delta$: 0.22 (s, 9H, $-C\equiv C-SiMe_3$), 3.2−3.6 (m, 2H, $-CH_2-$), 3.9−4.4 (m, 16H, $Fc_2$-*H*), 6.9−7.3 (m, 20H, Ph-H). $\delta_P$ ($CDCl_3$): 34 (s). **18:** From **13** (104 mg, 0.11 mmol), with ethyl acetate/hexane (2:5), gave after recrystallization from ethyl acetate, 53 mg (38%) of red-brown crystals of **18**. Anal. Calcd for $C_{64}H_{56}Co_2Fe_3O_4P_2Si$: C, 60.78; H, 4.46. Found: C, 60.04; H, 4.55. FAB-MS: *m/e* 1264 ($M^+$). $^1$H NMR ($CDCl_3$) $\delta$: 0.55 (s, 9H, $-SiMe_3$), 3.2−3.6 (m, 2H, $-CH_2-$), 3.8−4.3 (m, 25H, $Fc_3$-*H*), 6.9−7.3 (m, 20H, Ph-*H*). $\delta_P$ ($CDCl_3$): 34 (s). IR $\nu_{CO}$ (hexane): 2017, 2013, 1991, 1980, 1965, 1950 $cm^{-1}$. **19,20:** From **14**, eluting with ether/hexane (1:1), two major product bands were obtained. That with the highest $R_f$ gave red-brown **19** (21%). FAB-MS: *m/e* 1360 ($M^+$). $^1$H NMR ($CDCl_3$) $\delta$: 0.21 (s, 9H, $-C\equiv C-SiMe_3$), 0.55 (s, 9H, −cluster$-SiMe_3$), 3.2−3.6 (m, 2H,-$CH_2-$), 3.8−4.2 (m, 24H, $Fc_3$-*H*), 6.9−7.3 (m, 40H, Ph-*H*). IR $\nu_{CO}$ (hexane): 2017, 1991, 1965, 1950 $cm^{-1}$; $\nu_{C\equiv C}$: 2149 $cm^{-1}$. Removal of the second band gave red-brown crystalline **20** (41%). Anal. Calcd for $C_{98}H_{86}Co_4Fe_3O_8P_4Si_2$: C, 59.59; H, 4.39. Found: C, 59.33; H, 4.39. FB-MS: *m/e* 1974 ($M^+$). $^1$H NMR ($CDCl_3$) $\delta$: 0.56 (s, 18H, $-SiMe_3$), 3.2−3.6 (m, 4H,

$-CH_2-$), 3.8−4.2 (m, 24H, $Fc_3$-*H*), 6.9−7.3 (m, 40H, Ph-*H*). IR $\nu_{CO}$ (hexane): 2017, 1991, 1965, 1951 $cm^{-1}$.

**X-ray Data Collection, Reduction, and Structure Solution for 17.** Crystal data for **17** are given in Table 3. Recrystallization of **17** from ethyl acetate yielded red-brown blocks, one of which was used for data collection. Data were collected at 203(2) K on a Bruker SMART CCD diffractometer, processed using SAINT[24] with empirical absorption corrections applied using SADABS[25].

The structure was solved using SHELXS[26] and refined by full-matrix least-squares using SHELXL-97.[26] Non-hydrogen atoms were assigned anisotropic temperature factors, and the H atoms were included in calculated positions. Molecules of **17** lie on a center of symmetry located at the midpoint of the C−C bond of the fulvalenide ring system of the biferrocene moiety; refinement therefore involved only one-half of the molecular unit. A difference Fourier synthesis, following the location of all of the non-hydrogen atoms for **17**, revealed six substantial high peaks that could be readily assigned to ethyl acetate solvate in the crystal lattice. Anisotropic refinement of the solvate, with isotropic H atoms included as fixed contributions to Fc, led to a significant reduction in R1 and the absence of significant residual electron density in subsequent difference Fourier maps.

(24) *SMART (Control) and SAINT (Integration) software*; Bruker, AXS: Madison WI, 1994.

(25) *SADABS* (correction for area detector data); Bruker AXS: Madison WI, 1995 and 1997.

(26) Sheldrick, G. M. *SHELXS-96*; University of Göttingen: Germany, 1996. Sheldrick, G. M. *SHELXL-97*; University of Göttingen: Germany, 1997.

**Acknowledgment.** We thank Prof. W. T. Robinson (University of Canterbury) for the collection of X-ray data, the Uniiversity of Otago and the Royal Society (NZ) Marsden Fund for financial support, and Robinson College, Cambridge, for a Bye Fellowship (B.H.R.).

**Supporting Information Available:** X-ray data for **17** are available free of charge via the Internet at http://pubs.acs.org.

OM000493G